

# CNNtention: Can CNNs do better with Attention?

Julian Glattki

[jglattki3@gatech.edu](mailto:jglattki3@gatech.edu)

Nikhil Kapila

[nkapila6@gatech.edu](mailto:nkapila6@gatech.edu)

Tejas Rathi

[trathi9@gatech.edu](mailto:trathi9@gatech.edu)

[Github Repository](#)

## Abstract

*Convolutional Neural Networks (CNNs) have been the standard for image classification tasks for a long time, but more recently attention-based mechanisms have gained traction. This project aims to compare traditional CNNs with attention-augmented CNNs across an image classification task. By evaluating and comparing their performance, accuracy and computational efficiency, the project will highlight benefits and trade-off of the localized feature extraction of traditional CNNs and the global context capture in attention-augmented CNNs. By doing this, we can reveal further insights into their respective strengths and weaknesses, guide the selection of models based on specific application needs and ultimately, enhance understanding of these architectures in the deep learning community.*

## 1. Introduction

Convolutional Neural Networks (CNNs) have been the state-of-the-art architecture for image classification for many years and revolutionized the field of computer vision [1] [2]. Through convolution and pooling layers, CNNs are able to extract, preserve and structure spatial information, making them suitable for dealing with images. However, the architectural biases introduced through these layers force CNNs to rely on local receptive fields, thereby, among other limitations [3], hindering the networks from capturing long-range dependencies and global context [4]. More recently, Vision Transformers (ViTs) have taken over the leaderboards on image classification tasks (see [5] or [6]), showing the strength of attention-based mechanisms, which excel at capturing global relationships and thereby overcome some of the limitations of CNNs [7].

## 2. Background/Motivation

It is important to note that, even though Vision Transformers (ViTs) [8] are superior to CNNs and have taken over the leaderboards, there are certain limitations in ViTs

that deter its use such as requiring significant computational resources and since deep learning often involves trade-offs, it's crucial to factor this in when planning to deploy a solution especially on edge devices. Furthermore, ViTs require large datasets to learn well which makes it unsuitable for cases where we do not have large amount of data. This makes a strong case that combining the strength of both architectures can lead to a more robust and versatile model.

This idea has already been explored in the past. In [9], the authors employ Squeeze-And-Excitation blocks, which encode inter-channel relationships and thereby model channel-wise attention. The authors of [10] and [11] try a different approach by focusing on spatial features. Trying to tackle the shortcomings of these methods, the authors of [12] specifically focus on how attention-mechanisms can be used to model long-range dependencies. Newer papers, like [13] or [14], focus on the combination of these ideas and refine them further.

### 2.1. What are we doing?

We add 3 different attention mechanisms within a ResNet20 and observe how CNNs behave.

### 2.2. Novelty

While the effectiveness of attention has already been demonstrated across various CNN architectures and datasets by the respective authors. Our approach differs from previous works in mainly 2 ways:

- **Attention not added after every convolution:** We do not apply attention after every convolution operation as seen in [15] but rather after a sequence of different convolution operations. We do it this way to achieve an efficient trade-off which enables us to evaluate if we can add attentions with reduced computation overhead. In our architecture, we have added attention only 3 times in the full architecture as seen in [Figure 2](#).
- **No information given about positions:** We apply attention directly to convolutional layers without explicitly incorporating positional encodings unlike other approaches.

### 3. Datasets

#### 3.1. CIFAR-10

We use CIFAR10 dataset [16] as one of our datasets. Krizhevskii et al created the dataset as a reliably labeled subset of the 80 million tiny images [17] in order to show how semi-supervised learning and pre-training can improve classification models [18]. The 80 million tiny images dataset contained only weak labeled images scraped from the web, so a subset of semantically similar labels was corrected and filtered, resulting in a self-contained data set that consists of 60000 corrected, randomly-selected, colored and labeled 32x32 images with 10 classes of 6000 instances each, which show animals or modes of transportation. The creators already apply a 50k/10k train/test split, and we evaluate our models on the test set. For tuning, we employ a 45k/5k train/validation split and pick the best performing model. We reuse the data augmentation techniques introduced in [19], meaning that for the training set we randomly flip the images horizontally and take random crops of padded (with a padding of 4) versions of the images. Both the training and testing set are normalized based on values from [20].

#### 3.2. MNIST

We use the MNIST dataset [21], a standard benchmark which comprises of 70,000 grayscale images of handwritten digits (0-9), each sized 28x28 pixels. The data was originally collected by the National Institute of Standards and Technology and pre-processed to include resizing, normalization, and anti-aliasing. Pixel values represent intensity levels, and the dataset includes four incorrectly labeled examples [22]. For more details, refer to the dataset source.

### 4. Approach

For our baseline, we create an implementation of ResNet-20 (20 layers) inspired from [19].

#### 4.1. CIFAR-10 Baseline

First, we reduce the number of output channels in the initial convolution from 64 to 16 and adjust the kernel size, stride, and padding from 7, 2, and 3 to 3, 1, and 1, respectively. Second, we remove the subsequent max-pooling operation, as it is not mentioned in the paper. Third, we lower the number of residual stages from 4 to 3 and use output channels sizes of 16, 32 and 64. Fourth, in each residual block, when the spatial dimensions and number of channels increase, which applies identity mapping by padding feature maps with zeros to handle dimension mismatches. After experimenting with different variations we settled on the concise implementation shown in [23]. Lastly, we adjusted the final layer to 64 input features, as the final number of output

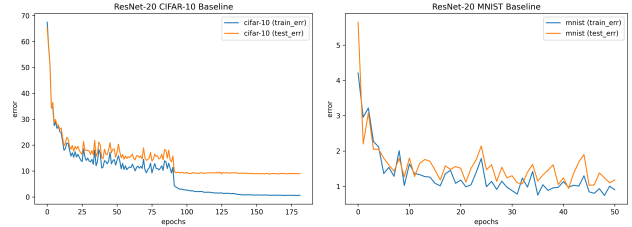


Figure 1: CIFAR-10 and MNIST ResNet re-implementation training/testing error.

channels is 64, and map these to the 10 classes of CIFAR-10. By training & evaluating the re implementation with the same hyperparameters mentioned in original paper (see Table 1), we achieve a test error of 9.04, closely matching the error of 8.75 mentioned in the original paper. Furthermore, as shown in Figure 1, when training the model on the entire training set as in [19], we achieve similar training and test error curves compared to the original papers.

Hyperparameter	Value
Batch Size and Epochs	128 batch size, 182 epochs
Learning Rate	0.1
Schedule (gamma=0.1)	Milestones: 91, 136
Optimizer and Momentum	SGD, 0.9
Weight Decay	0.0001

Table 1: Hyperparameters adapted from [19]. Milestones (91, 136 epochs) correspond to 32k and 48k iterations with a batch size of 128.

#### 4.2. MNIST Baseline

We extend the CIFAR-10 model to MNIST by changing input of initial convolutions from 3-channels to 1-channel and use it as our baseline model. Please note that the only reason we use MNIST is to ease our GradCAM [24] evaluations, baseline results in CIFAR-10 are sometimes confused between the spatial area of interest and background elements. By including a qualitative analysis with the cleaner 1-ch images of MNIST, we aim to provide a clearer evaluation of our experimentation.

#### 4.3. Attention

In this section, we shall lay the foundation by explaining where attention is being added and how attention is being implemented.

##### 4.3.1 The feature extractors

In our baseline implementation, the network is structured into sequential groups of residual blocks referred to as **layer 1**, **layer 2**, and **layer 3** in our code repository [25].

**Layer 1** extracts basic features like edges. **layer 2** reduces spatial resolution, captures mid-level features, and increases filters from 16 to 32 channels. **Layer 3** reduces spatial resolution and increases feature channels for deeper representation. This can be seen in detail in [Figure 2](#). We shall further refer to these layers as **Feature Extractors 1, 2, and 3**.

**But where to place Attention? A trade-off:** There is an interesting trade-off that plays out in our choice of adding the attention blocks between the feature extractors instead of within the feature extractors as seen in [Figure 2](#), i.e. after every convolution layer (within the residual blocks). It is seen in the CBAM paper [15] that adding attention between each convolutional layer could provide more control over feature importance.

While this may be true, we avoid this for 2 reasons:

- **Compute/time/memory:** Applying attention regularly increases computational and memory overhead.
- **Noisy features:** Features learned in the early layers may be noisy and not benefit from attention.

We let the feature extractors to create meaningful features and then add attention mechanisms to enhance these features.

### 4.3.2 Self-attention (SelfAtt)

The SelfAtt block enhances spatial relationships (along spatial axes) in feature maps by leveraging self-attention from [26] but in the context of images. We start by using 1x1 convolutions to project the input feature maps  $F$  into keys (K), queries (Q), and values (V) to create task specific representation of the input features as seen in [26] [27].

The block then computes raw attention scores (followed by softmax) by computing pair wise similarities which tells us how each spatial position attends to another spatial position. These scores are used to weight the values which combines relevant features across spatial positions.

$$\text{SelfAtt}(Q, K, V) = \text{softmax}(QK^\top) V \quad (1)$$

$$Q = XW_Q, \quad K = XW_K, \quad V = XW_V.$$

**Using 1x1 convs instead of linear layers:** While the original paper [26] uses linear layers to model Queries (Q), Keys (K), Values (V), using 1x1 conv firstly helps to preserve the spatial structure of our feature maps  $F$  and not lose it by collapsing it for a linear block.

**Similarity in information aggregation:** The 1x1 convolution in theory act similar to the global/avg pooling in CBAM ([subsubsection 4.3.4](#)). CBAM’s pooling aggregates spatial information globally for channel attention while 1x1 convolutions transform and mix channels locally at each spatial position for self-attention.

**Omission of  $\sqrt{d_k}$ :** In [Equation 1](#), we omit the scaling factor since the input channels (16, 32, 64) are small unlike embeddings in language models that are huge in comparison. Furthermore, omitting the scaling factor aids faster convergence as it would lead to stronger gradients.

### 4.3.3 MultiHead (Self) Attention (MHA) Block

We extend SelfAtt from [28] to MHA motivated from [26] which uses multiple heads to estimate attention features. We use 8 heads so that MHA can develop a distributed representation in hopes of better approximating long-term dependencies compared to SelfAtt.

$$\text{MultiHead}(Q, K, V) = \text{Concat}(\text{head}_1, \dots, \text{head}_h)W_O,$$

$$\text{where head}_i = \text{Attention}(QW_Q^i, KW_K^i, VW_V^i),$$

$$\text{Attention}(Q, K, V) = \text{softmax}\left(\frac{QK^\top}{\sqrt{d_k}}\right) V,$$

$$Q = XW_Q, \quad K = XW_K, \quad V = XW_V.$$

### 4.3.4 CBAM Block

Convolutional Block Attention Module (CBAM) [15] emphasizes meaningful features along two dimensions: channel and spatial axes. This module supports efficient flow of information within network by identifying features which should be suppressed and emphasized respectively. For the experiments here, channel attention and spatial attention are applied sequentially on a feature map as per below equations.

$$F' = F_c = M_c \times F$$

$$F'' = F_s = M_s \times F_c$$

$$M_c(F) = \sigma((MLP(F_{avg}^c) + MLP(F_{max}^c)))$$

$$M_s(F) = \sigma(f^{7 \times 7}(F_{avg}^s; F_{max}^s))$$

$F \in C \times H \times W$  is the feature map received from feature extractors as seen in [Figure 2](#).  $F_{avg}, F_{max}$  represents the global average and max pooled features.  $F_{avg}^c, F_{max}^c \in \mathbb{R}^{C \times 1 \times 1}$  are descriptors for channel attention, identified for all channel within feature map of size  $H \times W$ . This descriptors are forwarded to shared MLP to compute channel attention map  $M_c \in \mathbb{R}^{C \times 1 \times 1}$ .  $F_{avg}^s, F_{max}^s \in \mathbb{R}^{1 \times H \times W}$  are the descriptors for spatial attention, identified across channels on feature map of size  $H \times W$  which are concatenated and convolved through convolutional layer  $f^{7 \times 7}$  of kernel size 7 to produce spatial attention map  $M_s \in \mathbb{R}^{1 \times H \times W}$ . To reduce the number of parameters, number of perceptrons in shared MLP is controlled by a reduction ratio  $r$ , to produce hidden activation of size  $\mathbb{R}^{C/r \times 1 \times 1}$ . The hidden activation is followed by ReLU activation function [15].

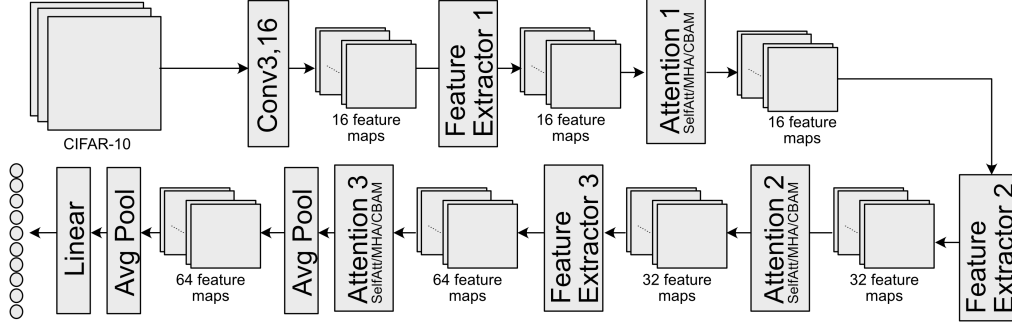


Figure 2: Overall architecture with attention added, the Feature Extractor layers are sequential blocks of convolutions that can be seen in [25]. Residual connections are not shown but exist between each feature extractor and attention layer as seen in Figure 7.

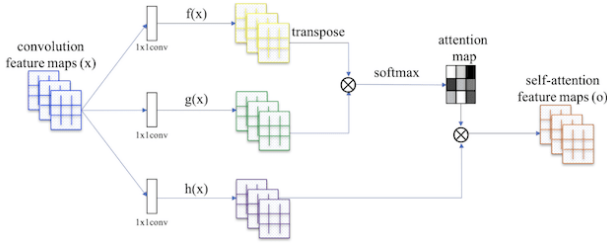


Figure 3: Self Attention module introduced in Self-Attention GANs. [28].

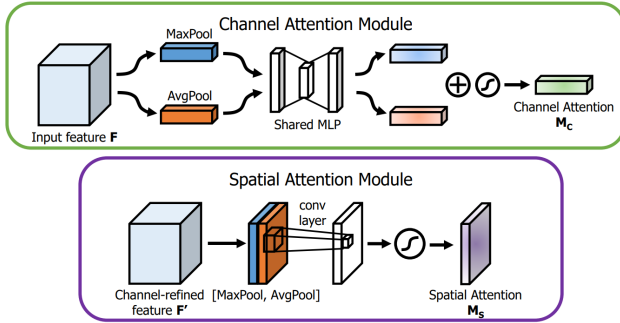


Figure 4: CBAM module introduced in [15].

**CBAM block placement:** Our implementation differs from the original paper [15] by adding the CBAM block after every residual block instead of within the residual block.

## 5. Experiments and Results

All our experimentation are recorded on MLFlow [29], an open source utility to track experiment runs. Please note that experimentation is done solely on CIFAR-10, we extend the best hyperparameters from CIFAR-10 to MNIST only for GradCAM observations as explained in subsection 3.2.

## 5.1. Experiments

### Optimizer changes, learning rate, regularization:

While SGD uses a more straightforward optimization path, Adam tends to converge faster and is more robust to hyperparameter choices due to its adaptive learning rates based on first and second moment of gradients. Apart from the optimizer, different experiments were ran for each model. We have mostly noted that model has a stable optimization path when learning rates are lower. We further play with regularization to achieve the best generalizable performance and employ EarlyStopping to save on computation costs. This can be seen in detail in our MLFlow results in our repo [25].

**The need for residual connections:** We initially train our models by using SelfAtt blocks without residual connections between the feature extractor layers, exactly as per Figure 2. However, this led to unstable training as seen in Figure 5. While attention mechanisms are powerful to capture long range dependencies, their contributions during the initial training stages may be limited as they are trying to build up effective representations of Q, K, and Vs.

$$R(x) = F(x) + x, \quad (2)$$

where  $F(x) = \text{SelfAtt/MHA/CBAM}$  for Equation 2

$$W(x) = w * F(x) + x, \quad (3)$$

where  $F(x) = \text{SelfAtt/MHA}$  for Equation 3

To address this, we introduce residual connections alongside the attention additions as seen in Equation 2, Equation 3, and Figure 7 which would help propagate information across the feature extraction layers and bypass the attention blocks when necessary. Over time as attentions begins to contribute meaningful representations, the residual connections would act as a stabilizing mechanism ensuring both direct and context information are leveraged efficiently.

This approach was inspired from [26] and is seen again

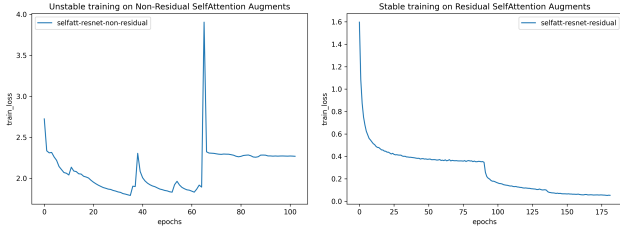


Figure 5: Stable training with (right) and without (left) residual connections between self-attention blocks.

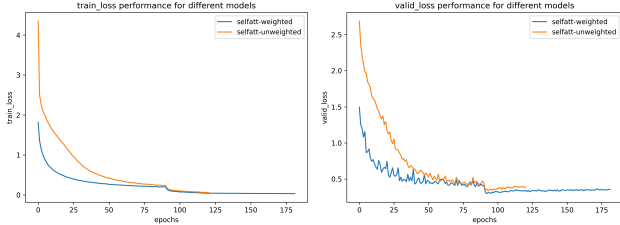


Figure 6: Faster convergence when SelfAtt model is allowed to select features dynamically.

in Vision Transformers (ViTs) from [8] wherein residual connections play a crucial role to stabilize training. While we see this aspect in Figure 5 for SelfAtt, we extend the same to MHA and CBAM.

**Model-Driven feature selection** Inspired from weighted residual concepts for deep networks [30], we train 2 models: with and without weighted attention as seen in Equation 3 and Figure 7.

The model converges faster when it is allowed to dynamically choose between output feature maps (from feat. extractors) and attention based features. During training we see the weighted version of the model has a higher validation accuracy of 90.01% as compared to 88.00%.

These weights being zero initially during training directly propagates the output feature maps. This is in line with our discussion from the residual connection section, i.e. self-attention takes time to build up meaningful representations [8] [26]. This is further evidenced in our plots where loss is lower for weighted model as seen in Figure 6.

**SelfAtt hyperparameters extended to MHA:** We use the tuned hyperparameters from SelfAtt for MHA as each head in MHA plays a role analogous to SelfAtt. Distribution of representation building across heads should reduce the optimization burden and ensures our comparison is solely due to architectural advantages in MHA.

**CBAM’s reduction ratio:** The reduction ratio controls the intermediate dimension of the shared MLP used in channel attention. A smaller reduction ratio has a large hidden layer, more parameters and in turn, higher capacity whereas a large reduction ratio has fewer parameters and lower ca-

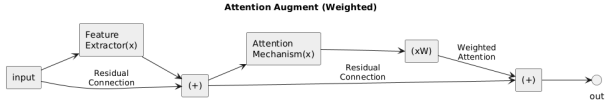
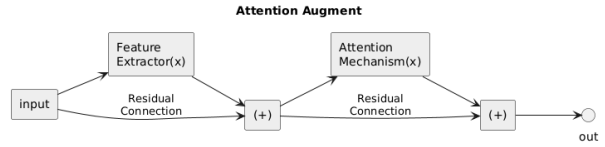


Figure 7: Attention added between feature extractor layers utilizing residual connections (top) and weighted residual connections (bottom).

CBAM-8	CBAM-16	CBAM-32
90.66%	90.32%	89.94%

Table 2: Comparison of performance on different  $r$  of CBAM’s attention block.

Model	CIFAR-10	MNIST	dur
Baseline	90.96%	98.52%	3.7h
SelfAtt	91.44%	99.30%	2.9h
MHA	91.06%	98.84%	5.1h
CBAM-16	91.32%	98.00%	1.8h

Table 3: Comparison of model performance on CIFAR-10 and MNIST datasets. Duration is on CIFAR-10 dataset only, MNIST has similar trends.

capacity. The reduction ratio  $r$  not only controls the parameter overhead but also how the channel attention block decides to propagate the output. This effect acts as a bottleneck, i.e. a higher reduction  $r$  leads to lower number of channels  $C/r$  which forces the MLP to retain the most useful information. In our experiments as seen in Table 2, we tune 3 models with different reduction ratios. We see that model performs similarly across different  $r$  with minuscule differences in performance. It means that the shared MLP is able to extract relevant information from the feature maps  $F$  even at lower capacities ( $r=32$ ). We strike a balance and pick a value of  $r = 16$ .

## 5.2. Results

We base our success on 2 criterion: (1) better or comparable performance to the baseline & (2) can our attention added models capture global dependencies?



### 5.2.1 Analysis of results

SelfAtt/MHA consistently outperform the baseline showing effectiveness of attention mechanisms on both datasets, i.e. SelfAtt/MHA maintain a better balance between local and global information compared to CBAM. CBAM’s final performance trails behind the other attention mechanisms and stabilizes to a higher test error compared to indicating less generalizable performance.

**Why CBAM trails against SelfAtt?** CBAM is highly focused on suppressing irrelevant feature maps through its shared MLP 4 and enhancing the critical areas, so this may cause over-suppression of areas of interest. Since CBAM combines 2 attention mechanisms sequentially (channel and spatial), this could also lead to bottleneck effects. To conclude, CBAM may excel at refining feature maps and suppressing irrelevant details but it can lead to loss of global context.

**CBAM’s efficiency trade-off:** It is important to note the trade-off here. While CBAM has comparable performance and in some cases is even better against baseline/SelfAtt/MHA as seen in Table 3, it is the fastest to converge. It shows faster convergence during the initial epochs as seen in Figure 8. Compared to SelfAtt/MHA, CBAM is lightweight, has lesser parameters to train (only a shared MLP and convolution layer), and hence, has lower computational overhead. To quantify this aspect, we use A-100s to train our MHA in 5 hours, training the same MHA on T4 would require 7.5-8 hours.

**GradCAM discussion:** Referring to dog image (first row) in Figure 9, we can see that SelfAtt effectively models global dependencies. The distributed representation approach in MHA tries to do as good as SelfAtt but it may be possible that each head in MHA learns different representations of Q, K, V which may not be as effective as a single head approach.

The CBAM’s channel block first finds the weighted output of the channels. These are used by the spatial block to highlight which parts of the image are important. Hence, CBAM identifies the important regions globally whereas SelfAtt/MHA identifies relationships between all positions. We can see this evidenced in Figure 9 where CBAM refines the baseline with sharper and effective features but SelfAtt/MHA does so with more granularity by capturing fine grained dependencies between positions (through pairwise computations).

As discussed in subsection 4.3.1, we theorized our models to only be able to refine what the baseline model is able to extract. The baseline can extract useful features when there is a contrast between the area of interest and background. There are examples when this is not the case as seen in the bird image (second row). To reinforce this idea, we take the MNIST dataset. In this case, each of models capture global dependencies more effectively as the base-

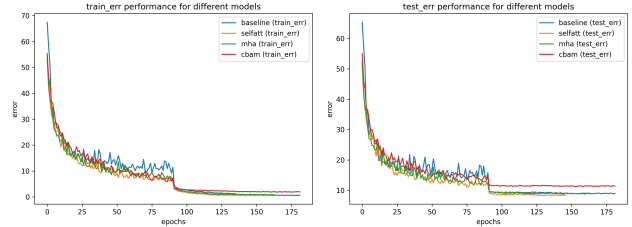


Figure 8: Train and test error on different models on CIFAR-10.

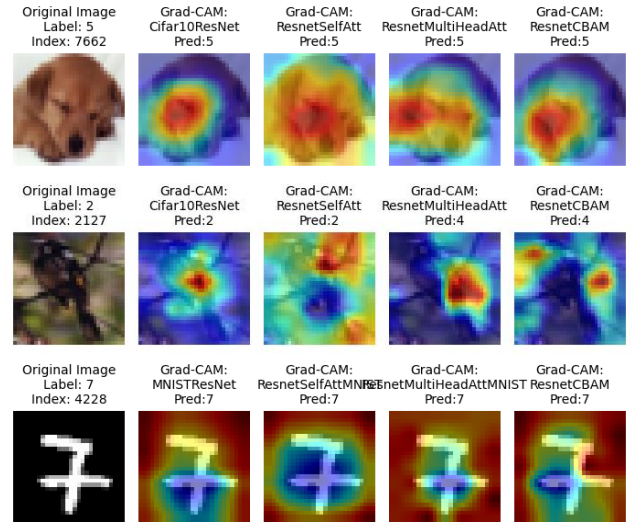


Figure 9: GradCAM results on CIFAR-10 and MNIST.

line model can extract better features. More such examples can be seen in Figure 10 and Figure 11.

### 5.3. Conclusion

We can conclude that CNNs indeed learn better when attention is added. This is proved by our quantitative and qualitative results. However, each attention mechanism has its own tradeoff to consider in regards to how they model global dependencies and the added computational overhead.

### 5.4. Related and Future Work

This work can be extended in many different directions.

- **Further study:** More study can be done to look at attention matrices in SelfAtt/MHA and what weights learn at different reduction ratios for CBAM. Furthermore, SelfAtt/MHA could be applied on both channel and spatial axes to make a 1:1 comparison with CBAM.
- **Parallel attention paths:** Inspired from GoogLeNet’s inception module [31], different attentions can be combined and concatenated to better approximate global

dependencies.

- **Train attention only:** One could freeze the baseline and only train attention to compare with our results.

## 6. Appendix

Here are more GradCAM results. We can see that the SelfAtt model captures long-range dependencies well. MHA's distributed head representation takes the baseline results and generates a more focused global context compared to the baseline. CBAM tends to enhance existing baseline closely with more sharper focus.

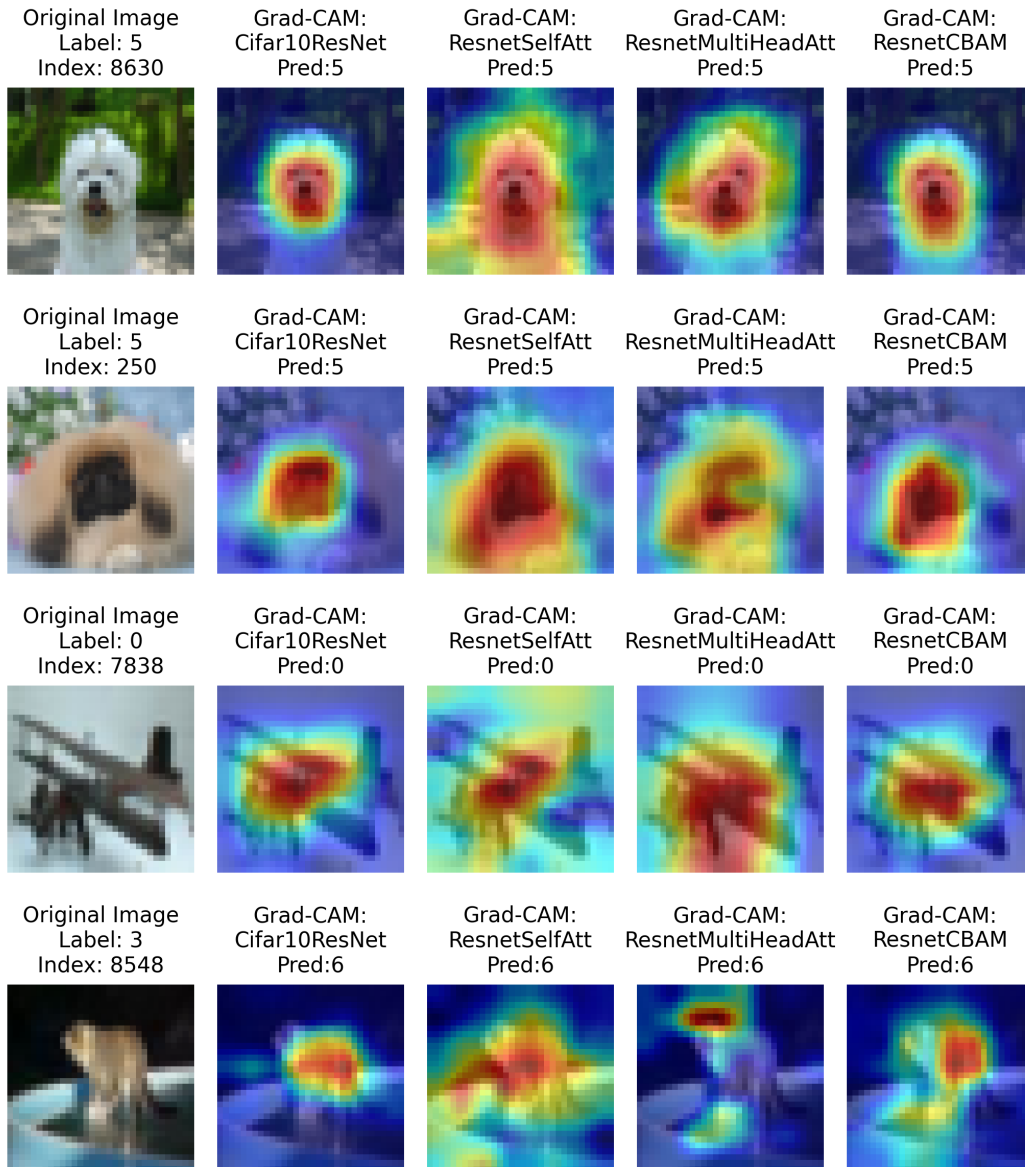


Figure 10: More GradCAM results on CIFAR-10 images.



For MNIST, we can see that the baseline model in all cases extracts relevant features. In a similar vein, the SelfAtt model tries to capture the global context whereas MHA's distributed representation tries to do it more effectively. Followed by the CBAM block that tends to enhance existing baseline results with more sharper focus.

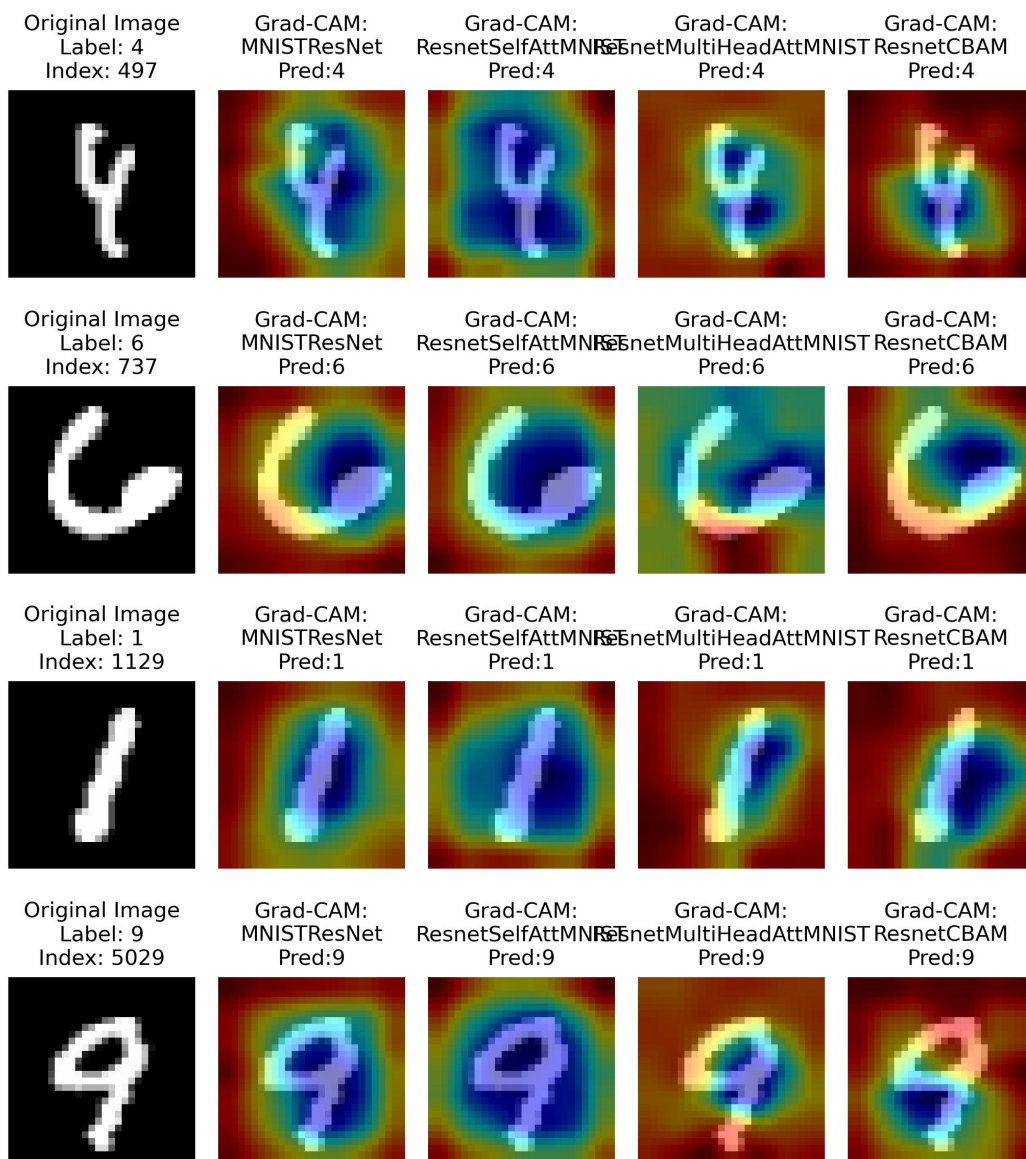


Figure 11: More GradCAM results on MNIST images.

## References

- [1] Waseem Rawat and Zenghui Wang. Deep convolutional neural networks for image classification: A comprehensive review. *Neural Computation*, 29(9):2352–2449, 09 2017. 1
- [2] Myeongsuk Pak and Sanghoon Kim. A review of deep learning in image recognition. In *2017 4th International Conference on Computer Applications and Information Processing Technology (CAIPT)*, pages 1–3, 2017. 1
- [3] Gabriela Rangel, Juan C. Cuevas-Tello, Jose Nunez-Varela, Cesar Puente, and Alejandra G. Silva-Trujillo. A survey on convolutional neural networks and their performance limitations in image recognition tasks. *Journal of Sensors*, 2024(1):2797320, 2024. 1
- [4] Ionut Cosmin Duta, Mariana Iuliana Georgescu, and Radu Tudor Ionescu. Contextual convolutional neural networks, 2021. 1
- [5] Xiaowei Yu, Zhe Huang, Minheng Chen, Yao Xue, Tianming Liu, and Dajiang Zhu. NoisyNn: Exploring the impact of information entropy change in learning systems, 2024. 1
- [6] Alexey Dosovitskiy, Lucas Beyer, Alexander Kolesnikov, Dirk Weissenborn, Xiaohua Zhai, Thomas Unterthiner, Mostafa Dehghani, Matthias Minderer, Georg Heigold, Sylvain Gelly, Jakob Uszkoreit, and Neil Houlsby. An image is worth 16x16 words: Transformers for image recognition at scale, 2021. 1
- [7] Maithra Raghu, Thomas Unterthiner, Simon Kornblith, Chiyuan Zhang, and Alexey Dosovitskiy. Do vision transformers see like convolutional neural networks?, 2022. 1
- [8] Alexey Dosovitskiy, Lucas Beyer, Alexander Kolesnikov, Dirk Weissenborn, Xiaohua Zhai, Thomas Unterthiner, Mostafa Dehghani, Matthias Minderer, Georg Heigold, Sylvain Gelly, Jakob Uszkoreit, and Neil Houlsby. An image is worth 16x16 words: Transformers for image recognition at scale. *CoRR*, abs/2010.11929, 2020. 1, 5
- [9] Jie Hu, Li Shen, Samuel Albanie, Gang Sun, and Enhua Wu. Squeeze-and-excitation networks, 2019. 1
- [10] Max Jaderberg, Karen Simonyan, Andrew Zisserman, and Koray Kavukcuoglu. Spatial transformer networks, 2016. 1
- [11] Ozan Oktay, Jo Schlemper, Loic Le Folgoc, Matthew Lee, Mattias Heinrich, Kazunari Misawa, Kensaku Mori, Steven McDonagh, Nils Y Hammerla, Bernhard Kainz, Ben Glocker, and Daniel Rueckert. Attention u-net: Learning where to look for the pancreas, 2018. 1
- [12] Yilin Liu, Xuezhou Guo, Xinqi Wang, and Fangzhou Du. Csanet: Channel spatial attention network for robust 3d face alignment and reconstruction, 2024. 1
- [13] Ran Gu, Guotai Wang, Tao Song, Rui Huang, Michael Aertsen, Jan Deprest, Sebastien Ourselin, Tom Vercauteren, and Shaoting Zhang. Ca-net: Comprehensive attention convolutional neural networks for explainable medical image segmentation. *IEEE Transactions on Medical Imaging*, 40(2):699–711, February 2021. 1
- [14] Wei Xu and Yi Wan. Ela: Efficient local attention for deep convolutional neural networks, 2024. 1
- [15] Sanghyun Woo, Jongchan Park, Joon-Young Lee, and In So Kweon. Cbam: Convolutional block attention module, 2018. 1, 3, 4
- [16] Alex Krizhevsky, Vinod Nair, and Geoffrey Hinton. Cifar-10 and cifar-100 (canadian institute for advance research). 2009. 2
- [17] Antonio Torralba, Rob Fergus, and William T. Freeman. 80 million tiny images: A large data set for nonparametric object and scene recognition. *IEEE Transactions on Pattern Analysis and Machine Intelligence*, 30(11):1958–1970, 2008. 2
- [18] Alex Krizhevsky. Learning multiple layers of features from tiny images. 2009. 2
- [19] Kaiming He, Xiangyu Zhang, Shaoqing Ren, and Jian Sun. Deep residual learning for image recognition, 2015. 2
- [20] Martyn A. Deep residual learning for image recognition: Cifar-10, pytorch implementation. <https://github.com/a-martyn/resnet>. Accessed: 2024-12-05. 2
- [21] Yann LeCun and Corinna Cortes. MNIST handwritten digit database. 2010. 2
- [22] Nicolas M. Müller and Karla Markert. Identifying mislabeled instances in classification datasets. pages 1–8, 2019. 2
- [23] Yerlan Idelbayev. Proper ResNet implementation for CIFAR10/CIFAR100 in PyTorch. [https://github.com/akamaster/pytorch\\_resnet\\_cifar10](https://github.com/akamaster/pytorch_resnet_cifar10). Accessed: 2024-12-05. 2
- [24] Ramprasaath R. Selvaraju, Abhishek Das, Ramakrishna Vedantam, Michael Cogswell, Devi Parikh, and Dhruv Batra. Grad-cam: Why did you say that? visual explanations from deep networks via gradient-based localization. *CoRR*, abs/1610.02391, 2016. 2
- [25] Tejas Rathi Julian Glattki, Nikhil Kapila. CNNtention Github Repository. <https://github.com/AttentionSeekers/CNNtention>, 2024. 2, 4
- [26] Ashish Vaswani, Noam Shazeer, Niki Parmar, Jakob Uszkoreit, Llion Jones, Aidan N. Gomez, Lukasz Kaiser, and Illia Polosukhin. Attention is all you need. *CoRR*, abs/1706.03762, 2017. 3, 4, 5
- [27] Irwan Bello, Barret Zoph, Ashish Vaswani, Jonathon Shlens, and Quoc V. Le. Attention augmented convolutional networks, 2020. 3
- [28] Han Zhang, Ian Goodfellow, Dimitris Metaxas, and Augustus Odena. Self-attention generative adversarial networks, 2019. 3, 4
- [29] Databricks. Mlflow: An open source platform for the machine learning lifecycle. 4
- [30] Falong Shen and Gang Zeng. Weighted residuals for very deep networks. *CoRR*, abs/1605.08831, 2016. 5
- [31] Christian Szegedy, Wei Liu, Yangqing Jia, Pierre Sermanet, Scott Reed, Dragomir Anguelov, Dumitru Erhan, Vincent Vanhoucke, and Andrew Rabinovich. Going deeper with convolutions, 2014. 6